Investigation of Standoff Distance Effect on Corrosion Behavior of Explosively Welded Joint between Two Aluminum Plates and Steel

M. R. Khanzadeh Gharah Shiran [*1], H. Bakhtiari [2], M. M. Ghafari [3], S. Rajaee [4], M. MohammadNejad [5]

[1] Center for Advanced Engineering Research, Majlesi Branch, Islamic Azad University, Isfahan, Iran
[2] Department of Materials Engineering, Science and Research Branch, Islamic Azad University, Najafabad, Iran
[3] Center for Advanced –Engineering Research, Majlesi Branch, Islamic Azad University, Isfahan, Iran
[4] Shahreza Branch, islamic azad University
[5] Department of Material Engineering, Shahid Bahonar University, Kerman, Iran

Abstract

In the present research, the effect of standoff distance on corrosion properties of the joint of three aluminum–steel explosive layers has been studied. For this purpose, the samples were welded with various standoff distance under constant explosive load. Optical Microscopy and Scanning Electron Microscopy were used to measure the quality of the joint and type of interface. Furthermore, point analysis of EDS was used to study the local and continuous welded areas. In addition, hardness test was employed to investigate the mechanics of the joints, electrochemical polarization and impedance in order to examine the corrosion behavior of various samples. Results of the microstructural investigations have suggested wavy – vortex transition of interface and formation of locally melted areas with a combination of the joined plates as a result of standoff distance and collision kinetic energy augmentation. Results indicated that changes of iron percentage rate in localized fusion areas of the interface had considerable effect on the cathodic behavior and corrosion caused by the galvanic cell of the interface. Moreover, the increase of collision kinetic energy in the interface led to a decrease in corrosion resistance in the impedance test.

Keywords: Collision kinetic energy; Explosive welding; Galvanic couple; Standoff distance; Local fusion areas.

1. Introduction

In explosive welding method, controlled energy of an explosive material is used to place the welded surfaces in a determined standoff distance against each other to approach and collide at a high speed. As a result of the collision of the two surfaces, a local pastry field is established in the joint interface. By sharing the electrons, a band with metallurgical bond is set up among the welded parts. Due to a high collision pressure, one jet with a high speed is formed from two joint surfaces leading to the establishment of clean joining surfaces in the welding interface and elimination of surface pollutions. Formation of this jet is one of the basic conditions of establishment of appropriate bond in the explosive welding. This welding process is a not-fusion importance, and out of its industrial applications, it can be referred to as bonding and cladding of the diversified homogeneous and non–homogenous metals in the form of two or a few layers.

** Corresponding author*
Email: M.khanzadeh@iaumajlesi.ac.ir
Address: Center for Advanced Engineering Research, Majlesi Branch, Islamic Azad University, Isfahan, Iran
1. Assistant Professor
2. M.Sc.
3. M.Sc.
4. M.Sc.
5. M.Sc.

According to the absence of significant heating during this process, the welds performed by this method do not have considerable negative characteristics compared to the parts bonded by fusion, hot rolling or warm forging welding processes [1-4].

A limited number of researches have been conducted to study the corrosion of explosive joints. Some of these references are mentioned in this section. Kengkla and Tareelap [5] have studied the effect of intermetallic compounds on corrosion behavior of joints of three aluminum/steel explosive layers in military applications. They reported that the formation of Al_3Fe and Al_5Fe_2 intermetallic compounds in the joint interface led to the establishment of the cathodic state towards aluminum and anodic state towards steel. As a result, the desired corrosion attack was achieved next to the boundary of aluminum and intermetallic compounds. Mudali et al. [6] studied corrosion of explosive joint of titanium and type 304 stainless steel. Their results indicated that flexible strength of joint in the Nitric acid medium was in the standard limit, and corrosion attack concentrated mainly on the interface of joint. Acarer [7] investigated corrosion of explosive joint of aluminum and copper. Results indicated that galvanic corrosion occurred in the joint, and aluminum side of the joint showed to have higher anodic state because of higher electronegativity. Therefore, the corrosion in aluminum side was higher compared to the copper side. Kahraman et al. [8] studied corrosion of explosive joint of titanium and stainless steel. Results showed that in the corrosive environment, the mass of joined plates increased on the surface due to more intense plastic transformation and formation of the oxide layer with the increase of the explosive load. In addition, corrosion of explosive joint in the Ti–6Al– 4 V and aluminum plates was investigated. Results of the corrosion test revealed that the weight loss rate of materials increased at the beginning of the corrosion tests, and then it decreased [9]. Furthermore, the increase of plastic transformation rate caused by the increase of explosive load rate led to intensification of the samples weight loss in the corrosion test. Zareie et al. [10] studied a comparison of corrosion behavior between fusion and explosive joint of Inconel 625 and plain-carbon steel. Their results showed that resistance to corrosion of joint was more uneven in the fusion welding, which was due to chemical heterogeneities caused by micro-isolation and establishment of the secondary destructive phases and their accumulation in fusion joint, which contributed to the formation of a stable passive layer.

Studying the explosive joint of three thick layers of $AlMg_5$, pure aluminum and steel alloys by placing emphasis on interface of none- homogenous joint of aluminum and steel, and the effect of different parameters including standoff distance and explosive load on the metallurgical and mechanical properties of the interface of this non-homogeneous joint is a novel problem which is worth investigating; therefore, it is considered in this article. Whereas this welding compound is intensely used in marine areas and superstructures of ships, the study of corrosion properties can prevent failure.

2. Experimental Methods

2. 1. Raw material

2. 1. 1. The used alloys

A (310 mm × 260 mm × 7 mm) 5083 aluminum plate , a (305 mm × 255 mm × 10 mm) 1050 aluminum plate and a (300 mm × 250 mm × 20 mm) steel plate were considered as the flying and intermediary plates, and the plain-carbon steel plate was considered as the base plate.

In order to weld Mg-Zn-Al alloys to steel, the use of a pure aluminum intermediary layer was suggested in order to establish a proper connection bond due to extensive freezing limitation and relatively low density of the alloy. This was due to higher melting point, freezing amplitude close to zero, higher thermal conduction of aluminum and decreasing rate of melted phase formed in the interface of aluminum/steel joint. Out of the aluminum alloys, the AA1050 alloy was selected as the intermediary layer in order to minimize intermetallic compounds of the interface. Mechanical and physical properties of the used alloys are illustrated in Table 1 [11].

Table 1. Mechanical and physical properties of the used alloys.

Speed of sound (m/s)	Fusion temperature(ºC)	Elastic module (GPa)	Poisson coefficient	Hardness (MPa)	Hardness (HV)	Yield Strength (MPa)	Density (kg/m3)	Materials
4804	1540	210	0/3	1765	160	355	7850	AISI 1515
4996	1540	69	0/33	294/2	30	100	2710	AA1050
5090	570	70	0/33	804	82	320	2660	AA5083

Following the sandblast and rust cleansing, metals were papered and polished to be completely clean. Following this, the plates were washed first by CaOH solution and ethanol 95%, then by water and finally, dried

ANFO explosive material which is a mixture of ammonium nitrate, rbonaceous materials and gasoline liquid fuel, was provided by the mixture of 94.5% ammonium nitrate and 5.5% of gasoline.

Besides, in order to conduct explosion process of this material, M8 detonator was used. In Table 2, characteristics of tests and nomination of the samples have been reported by providing the corresponding intervals and parameters. Parallel array system on the concrete platform with a bed of soft sand as the buffer and intermediary layer were used to perform the placement of samples (see Fig. 1). M8 detonator has been used to stimulate according to the placement in Fig. 1. The speed of explosive materials was measured by making use of fiber optics by the speedometer.

2. 1. 2. Experimental investigations

In order to conduct the metallographic test, the samples were provided with the dimension of one cm by photomicroscopy. Following the sand papering and polishing by diamond paste for the purpose of microstructural investigation of the samples steel section, they became etched in 2% Nital solution. Moreover, the test of the scanning electron microscope was conducted by microscope, VEGA TESCAN model, which is equipped with EDS analysis system. In this research, micro hardness test was conducted based on Vickers according to ASTM 384-11 standard. The exercising force of 2.200 gram per 20 seconds was implemented 12). By sketching the Nyquist curves obtained by EIS test, electrochemical tests were conducted in this study using Potensastate apparatus, (Model of Auto LAB –AUT8) in 3.5% NaCl solution within a frequency range of 100 KHz to 10 MHz once the samples reach stable state (changes were less than 5 mV per 5 minutes). During the test, three-electrode cells were used. In this step, SEC calomel saturation electrode and platinum electrode were used as the reference electrode and aiding electrode respectively. Corrosion behavior was studied using dynamic potentiation polarization test. This test, with calomel saturation reference electrode, was conducted in 1000 m/l solution of distilled water in the presence of 35 grams NaCl and PH=6.8 in the Voltage range of -1 to 1 towards OCP via scan speed of 1 m v/s and under room temperature on all samples.

The samples were floated in the solution for 30 minutes so that acceptable stability was achieved. Following this, values of corrosion potential (Ecorr) were calculated using the obtained diagrams, density diagram of corrosion current (Icorr) and Tafel extrapolation method.

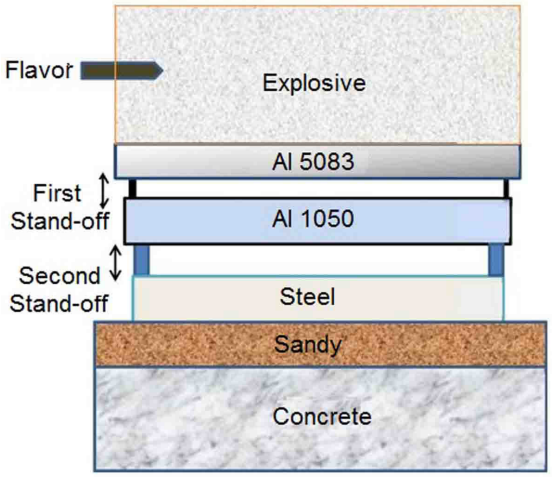

Fig. 1. Regulation of explosive tests.

2. 1. 3. Immersion test

Having weighed the samples up to four decimal places, the samples were naturally immersed in aerated, non-agitated NaCl solution for 1000 hours based on ASTMG31 standard 13). According to ASTM G71 standard, 40 ml of solution was prepared for any square centimeter of the submerged sample surface area. The reduction in solution volume, which occurred due to evaporation during the process, was compensated by distilled water 14). In weight loss analysis, joint sections were prepared and weighted. Then, they were immersed in the solution.

Table 2. Parameters of the designed tests.

Test No.	Diameter of explosive material (mm)	Standoff distance between base plate and intermediary plate (mm)	Standoff distance between flying plate and intermediary plate (mm)	Explosive ratio
A	50	8	10	2/41
B	50	10	10	2/41
C	50	10	6	2/41

After 1000 hours, the corrosion product layers were removed, the samples were re-weighted, and weight losses and corrosion rates were calculated.

3. Results

3. 1. Microstructural studies

In explosive welding, two molten interfaces including "metal to metal" and "metal to frozen" can be achieved at the interface. In addition to a minimum speed of the flying plate, there is a minimum value of the collision kinetic energy for joining.

As a result of the collision of flying plate, the consumed kinetic energy converts into potential energy, which led to deformation of collision surfaces. If the plastic deformation was not sufficient, short waves were established; therefore, local fusion area did not appear. As observed in Figs. 2. and 3, the interface of aluminum-steel joint is asymmetrical wavy – vortex based on two major reasons. Firstly, due to density difference between two alloys. Secondly, due to the considerable standoff distance between the aluminum plates.

Higher collision speed of the flying plate made higher kinetic energy be transferred to the second interface, and as a result, a wave and vortex-shaped interface was established. With the increase of collision kinetic energy, an intense transformation was established at the bottom and top of wave. As a result of high collision pressures, the vortexes could be established in the interface of joint, and these vortexes might create local fusion areas in some interface areas. The internal heat generated on the basis of a high pressure resulted from the shock wave of explosion and intense plastic deformation. Besides, generation of adiabatic heat due to getting vortex caught in the frontier of some waves might be contributed to the transformation of kinetic energy into thermal energy during collision or adiabatic heat caused by the gases trapped between the plates. These local areas were surrounded by the cold metal and subjected to high cooling rates in the range of 105 to 107 k/s [15, 16]. These small areas were observed in the vicinity of the vortex of waves in Figs. 2 and 3.

With the increase of standoff distance or rate of explosive load due to the increase of collision pressure and the consequent energy and temperature, the rate of these areas in the interface, especially in the vicinity of the vortex of waves increased. Since the shape of the waves were not completely symmetrical because of the differences in density and speed of wave dissemination within the two metals, and the fact that Thermal conductivity

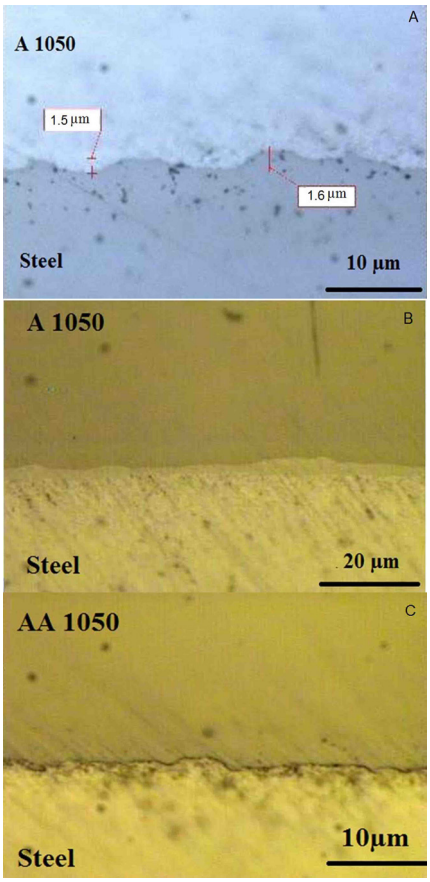

Fig. 2. Photo metallographic pictures of the interface of middle aluminum to steel A: sample A, B: sample B, C: sample C.

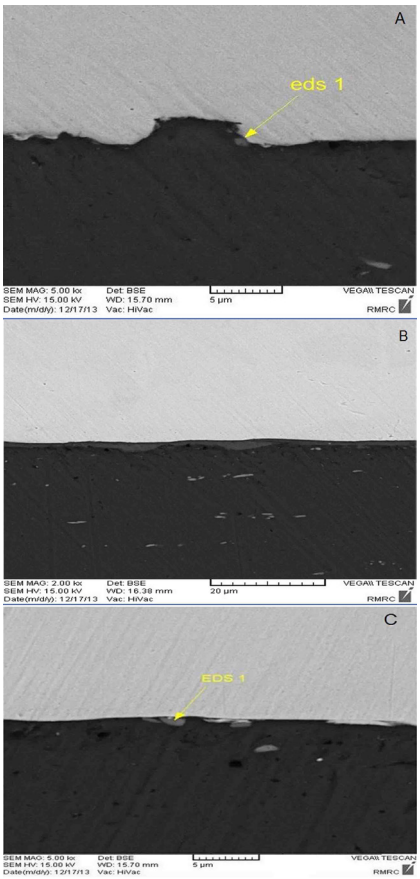

Fig. 3. Pictures of scanning electron microscope of aluminum/steel interface. A: sample A, B: sample B, C: sample C.

of steel is lower than aluminum, these compounds have been concentrated in one direction of waves during the cooling process and were observed in sample B in order to transfer more heat in the direction of steel. The effect of thermal conductivity of welded metals on the concentration of local fusion areas was not in accordance with the results reported by Liaghat and Hokamoto [17, 18]. Results of EDS analysis of the scanning electron microscope related to the local fusion area in front of the vortexes are illustrated in the Fig. 4.

Results of these analyses suggest the establishment of a mixed compound of two alloys in these local areas based on turbulent and rotational motion of the caught jet consisting of two base and flying plates in these areas. Formation of the jet from these plates and its rotational motion were observed by Hokamoto [8], Kahraman [14] and Akbari Mousavi [18]. Moreover, results indicated that the analysis of these compounds at various waves experiences significant changes with the change of welding parameters, so it was not homogenous [16-21].

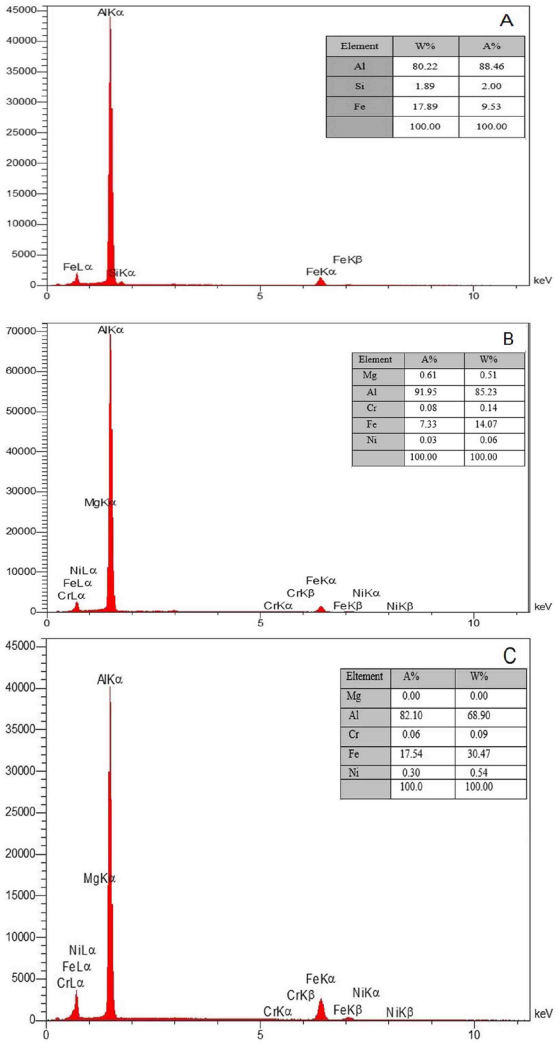

Fig. 4. Results of EDS analysis from local fusion area of aluminum/steel joint. A: sample A, B: Sample B, C: sample C.

3. 2. Microhardness assessment

Fig. 5 shows the results obtained by micro hardness test in the vicinity of 1050 aluminum/ steel and 1050 aluminum/ 5083 aluminum interfaces in various samples. It can be observed that hardness of the intermediary aluminum plate in the vicinity of aluminum/aluminum interface is higher than the distant areas because of the high transferred kinetic energy caused by the collision of two aluminum plates at the interface in comparison with the areas distant from the interface. This issue was reported by Benak [3], Kengkla [5] and Acarer [7]. Obviously, in this part of the aluminum sheet of the intermediary plate, the returned waves caused by explosion shock of anvil surface did not have considerable effects because of travelling a long path. In all test samples, hardness in the section of steel and aluminum next to 1050 steel/ aluminum interface was higher compared to distant areas.

During the conducted studies, this was due to transferring energy caused by the collision of two sheets of intermediary plate aluminum and steel sheet while performing explosive welding process. In addition, return of the shock waves resulted from explosion of anvil surface towards upper direction and getting close to the mentioned interface could be mentioned as the other contributor. On the one hand, according to higher hard work

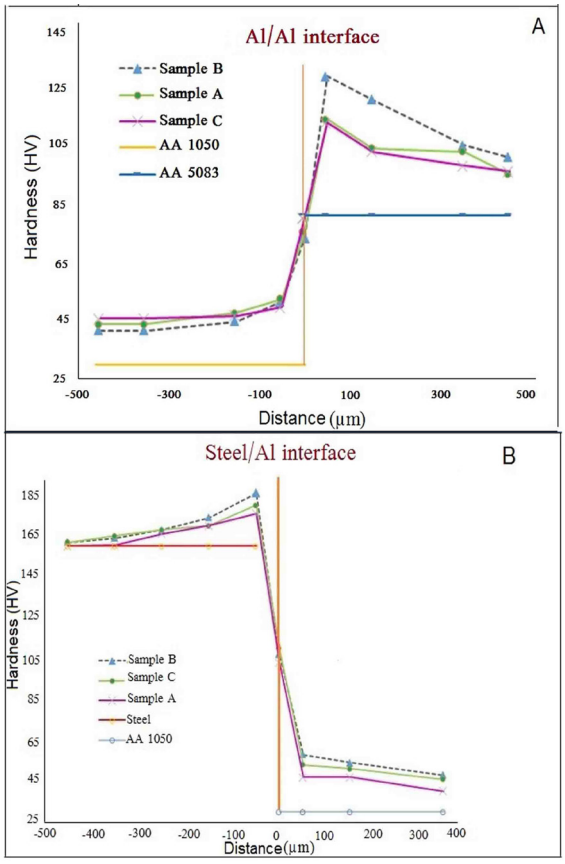

Fig. 5. Results achieved from micro hardness test. A–5083 aluminum / 1050 aluminum interface B–1050 steel/ aluminum interface.

rate of the steel layer compared to aluminum layer, the increase of hardness in the steel part was lower than the other direction.

Comparison between Fig. 5-A and 5-B reveals that the rate of hardness announced for part of interlayer plate aluminum in the vicinity of aluminum / steel interface was higher than the rate of the hardness of similar part in proximity of aluminum/ aluminum interface. Because interlayer was close to anvil surface , which led to more return of the reflected shock waves from surface of anvil to steel/ aluminum interface.

According to the hardness profiles in Fig. 5-A and comparison of hardness in the vicinity of aluminum / aluminum interface of two test samples No A and B, it was observed that despite the equality of the first standoff distance among the aluminum plates in both mentioned samples, hardness figure in the test sample No. B was higher than No. A. A more accurate investigation revealed that it was firstly due to the short wary interface in sample B against flat wavy interface of sample A. Secondly, it was contributed to the increase of the second standoff distance between aluminum sheet of intermediary plate and steel sheet, and the effect of collision energy increased while carrying out the fusion because of higher standoff distance. Similarly, by comparing hardness in the vicinity of aluminum/ steel interface of the two test samples No. A and B, it was also observed that due to the increase of standoff distance between the two mentioned sheets, and as a result of the increase of transferring kinetic energy while performing the fusion process, also by considering the shape of mentioned interface in sample No. B in wavy form along with perpetual local fusion bond leading to establishment of interference of waves and higher transfer of kinetic energy to the mentioned interface, hardness figure in two directions of the second interface in the test sample No. B was higher than test sample No. A.

According to the hardness profiles in Fig. 5-A and 5-B, by comparing two test samples No. B and C in interface among aluminum plates, it was observed that the rate of hardness along aluminum /aluminum interface in 5083 part increased at the same ratio considering the higher first standoff distance among aluminum plates in sample B compared to sample C. However, in the section of intermediary plate aluminum of both test samples, the mentioned hardness figure was the same in both test samples approximately considering the effect of the second standoff distance, shape of aluminum / aluminum and aluminum / steel interfaces, and also the existence of attached bond of local fusion in sample No. B. According to the hardness figure in two directions of aluminum / steel interface in these two test samples, hardness figure in sample No. B in the steel plate was higher than sample No. C.

3. 3. Immersion testing

The results of weight loss analysis for the samples are listed in Table 3. Initial weights of the samples are also included in this table. Anodic reaction was distributed throughout the surface due to the high energy of explosive welding process induced by sever plastic deformation. The highest and the lowest weight losses were associated with sample C and sample B respectively. As a result, sample C had the highest corrosion rate. The kinetic energies of interface grew as stand-off distances increased. Therefore, kinetic energy growth along with severe plastic deformation results in a uniform film formation in sample B as well as local melting of sample C. EDS analysis of sample B (Fig. 4) demonstrate that the obtained compound had a lower amount of Fe, so it showed less cathodic behavior compared to aluminum cases and the other samples. The galvanic cell formed between aluminum and steel, resulted from the continuous molten band, was less likely to form another galvanic cell at the Al/steel interface. Therefore, the weight loss in sample B was the lowest, and its corrosion resistance was higher than the other two samples. Considering the EDS analysis of sample C, these areas contained $FeAl_3$ compounds, setting up a secondary galvanic cell with aluminum, apart from the galvanic cell firstly formed between aluminum and steel. This secondary galvanic cell increased the current density as well as corrosion rate, which led to the reduction of its corrosion resistance more than two other samples.

Table 3. Weight losses and corrosion rates after immersion in the solution for 1000 hours.

Sample	C.R. (mpy)	I_{corr}(μA)	E_{corr} (mV)
1050 aluminum	0/89	1.62	-735
raw steel	5.14	9.32	-612
Sample A	2.4	4.35	-698
Sample B	1.75	3.18	-693
Sample c	2.5	4.55	-711

3. 4. Polarization electrochemical test

Fig. 6 describes polarization behavior of 1050 aluminum, steel and welded samples. The parameters obtained from these diagrams, such as amount of corrosion potential (Ecorr) and density of corrosion current (Icorr) using Tafel extrapolation method are shown in Table 4. Moreover, a more accurate observation of the obtained diagrams in Fig. 6 revealed that the anodic branch of the polarization curves of 1050 aluminum, steel and various areas of the weld were similar. This meant that aluminum, steel and different areas of weld had an anodic dissolution mechanism. On the other hand, it was observed that cathodic branches were approximately similar in all diagrams. On the other hand, mechanisms of the cathodic branch of these curves were the same, which meant that cathodic reaction was controlled by activation, namely reaction of water and oxygen reduction. Therefore, according to the polarization curves of various areas of the weld, it was noted that corrosion of these areas was under control of the cathodic reaction because Tafel cathodic slope was higher than its anodic slope.

From Table 4, it can be inferred that corrosion and potential density of corrosion current were various in weld areas between steel and 1050 aluminum. It means that the tendency for corrosion of various weld areas was less than aluminum but higher than steel. In contrast, the intensity of corrosion current density of various weld areas was less than steel but higher than aluminum.
Therefore, the corrosion rate resistance of these regions was higher than the steel.

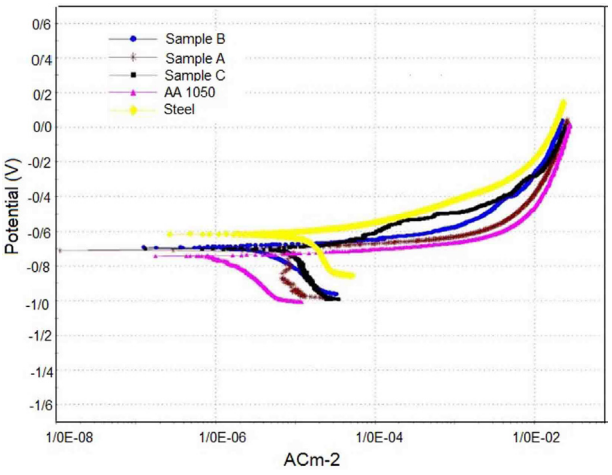

Fig. 6. Polarization behavior of aluminum, steel and welded samples.

Fig. 7 showed optical micrographs of the welded joints followed by Immersion test. As can be observed in the micrographs, corrosion of sample B is obviously less than other two samples.

Corrosion behavior mechanisms of aluminum and steel can be summarized as follows:
For steel, the cathodic reaction, which occurred on the surface, was oxygen reduction, and the anodic reaction was metallic ionization. However, the mechanism in the voids would be different. Having triggered anodic reaction of metal ionization, the resultant metallic ions were hydrolyzed by water molecules. Following this, the produced hydroxides reacted with the Cl ions immigrated into the voids and, as a result, iron chloride was produced.

$$O_2 + 2H_2O + 4e \rightarrow 4OH^- \quad (1)$$

$$Fe \rightarrow Fe^{2+} + 2e \quad (2)$$

Similarly, for aluminum, the cathodic reaction which occurred on the surface was oxygen reduction, and the anodic reaction included aluminum ion generation.

$$Al \rightarrow Al^{3+} + 3e \quad (3)$$

The mechanism that occurred in the void was different from surface reactions. Hydrolysis of aluminum ions and hydrogen production as the cathodic reaction as well as the migration of hydrogen ions out of the cavity determined the pH of the cavity. Under the produced pH, aluminum hydroxide was synthesized. Similar procedure was followed for aluminum hydroxide reproduction [22, 23].

Table 4. Results achieved from polarization diagram.

Sample		R_{ct}	n_{dl}	Q_{dl}	R_f	n_f	Q_f	R_s
Base metal of aluminum		34.41	0.81	1.59	83.12	0.83	1.44	33
Base metal of steel		11.93	0.74	5.82	44.2	0.73	3.84	26
Sample A		23.87	0.81	2.04	63.41	0/81	1.65	29.4
Sample B		17.12	0.76	3.62	55.13	0.78	1.86	24.3
Sample C		18.31	0.73	4.14	53.22	0.71	2.34	24.9

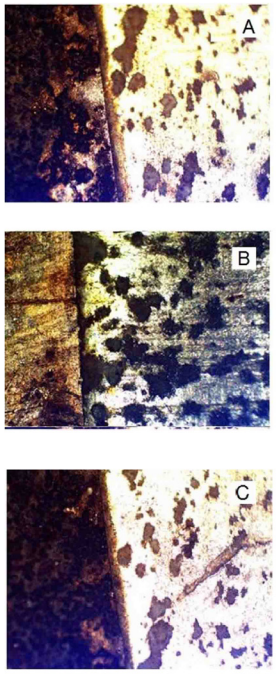

Fig. 7. Optical micrographs of the welded joints, followed by Immersion test; A) sample A, B) sample B, and C) sample C.

It should be noted that when weld areas in solution were tested, two types of galvanic couples appeared. One of them was observed between aluminum and steel, and the other appeared between local fusion areas containing iron and aluminum ground. According to Fig. 2, one adjacent fusion bond appeared in the aluminum/ steel interface within sample No. B due to highness of standoff distance and collision kinetic energy caused by shock waves. EDS analysis of this area in Fig. 4 indicates that the established compound contained less iron; thus, it showed less cathodic behavior towards aluminum ground and had a less inclination towards establishment of another galvanic cell in the aluminum/ steel interface compared to other two galvanic cells achieved between aluminum/ steel resulted from attached fusion bond. Based on this reason, corrosion speed was lower in sample B and. Therefore, the corrosion resistance of this sample was higher than the other two samples. Studies and observations of Kengkla [5], Acarer [7], and Zareie Rajani [10] also confirmed this observation.

For sample C, the wave amplitude drop owning to the reduced collision kinetic energy transferred to the steel-aluminum interface, induced by decreased stand-off distance between aluminum plates. However, locally-melted regions were fabricated at the interface due to the large stand-off distance between aluminum and steel. Considering the EDS analysis, these regions constituted $FeAl_3$ compounds, setting up a secondary galvanic cell with aluminum in addition to the galvanic firstly formed between aluminum and steel. This secondary galvanic cell increased the current density as well as corrosion rate, which led to reduction of corrosion resistance more than the other two samples. Moreover, it is well known that the non-equilibrium potential of aluminum and steel are -1.66 V (SCE) and −0.44 V (SCE) in the 3% NaCl solution, respectively. The nonequilibrium potential of iron is more than +122 mV to that of aluminum; and the corrosion resistance order is Fe> Al. Therefore, it was sure that the potential of the Al-rich phases moved to negative direction.

According to sample A, since the stand-off distances between aluminum layers were large enough, the collision kinetic energy transferred to the steel-aluminum interface increased. However, locally-melted regions with lower dimensions were fabricated at the interface due to the reduced stand-off distance between steel and aluminum. Although these regions allowed the formation of secondary galvanic cell with Al matrix, the corrosion rate induced by galvanic cell was lower due to the smaller surface area of the regions. Therefore, the current intensity and corrosion rate of sample A was lower than that of sample C and considerably a better corrosion resistance was achieved.

The locally-melted regions containing Fe atoms showed cathodic behavior relative to the Al matrix. These regions were susceptible to the oxygen reduction cathodic reaction. Therefore, the cathodic and anodic reactions in these reigns were oxygen reduction and aluminum oxidation respectively. As a result of oxygen reduction reaction, the solution PH locally rose in these regions, and in view of the existing alkaline environment, the Al matrix was dissolved in neighboring areas.

3. 5. Electrochemical impedance (EIS)

Equivalent circuit used to analyze the data obtained by electrochemical spectrometry test is illustrated in Fig. 8. In this circuit, R_s, Q_f, R_f, Q_{dl} and R_{ct} represent resistance of solution, constant phase element (CPE) in the surface film, the resistance of the surface film, constant phase element in the dual layer and transferring resistance of the load respectively.

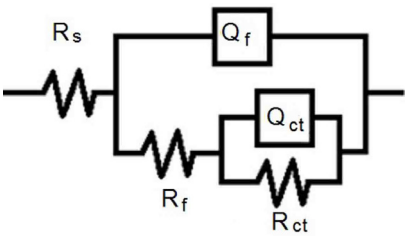

Fig. 8. Equivalent circuit used in the analysis of the EIS data.

Diagrams of aluminum–steel electrochemical impedance and weld areas are illustrated in Fig. 9. Fig.

10 shows the phase Bode diagrams of the base metals and samples. Table 5 illustrates the data obtained from the correspondence of R (Q (R (QR)) equivalent circuit with EIS result. In Table 5, frequency power (n_f) suggests the rate of compression of the surface film. When the compressed surface film approaches one, and with the increase of this figure, corrosion current decreases. From results of the electrochemical impedance test, it can be inferred that sample A had the highest surface film resistance (R_f) and load transfer resistance (R_{Ct}) compared to samples B and C. In other words, according to the fact that the iron rate in the aluminum and steel interface of samples A and B was lower compared to sample C as seen in Fig. 4, and the less tendency to establish galvanic cell in the aluminum/ steel interface made them enjoy a higher corrosion resistance compared to sample C. Due to the increase of standoff distance of sample B and increase of collision kinetic energy transferred to interface, this sample was of a lower corrosion resistance compared to sample A. Results of polarization and impedance indicated that sample C has the lowest corrosion resistance. In the research by Zareie Rajani and Khanzadeh, these results were provided [10-24].

4. Conclusion

In this research, investigation of corrosion behavior and microstructural changes of explosive plates of plain-carbon steel, aluminum 5083 and aluminum 1050 were conducted considering standoff distance in marine environment. Results can be summarized as follows:

- According to the differences in density of aluminum and steel alloys and the large standoff distance between the aluminum plates, more collision kinetic energy was transferred to the second interface. This led to creation of wavy interface as well as increased locally-melted regions.
- Owing to shock hardening effect, the transferred collision energy caused by the explosion waves of two aluminum plates to the Al/Al interface as well as receiving the upward-reflected waves at the steel/1050 aluminum interface, induced by the explosion at the anvil surface, the hardness in the vicinity of interfaces was higher than other points.
- With the decrease of Al/steel standoff distance along with locally melted regions at the interface, corrosion rate caused by resultant galvanic cell dropped. This led to reduction in current intensity and corrosion rate, and enhancement in corrosion resistance.
- According to the EDS analysis results, in addition to the galvanic cell, firstly formed between aluminum and steel, presence of $FeAL_3$ compounds in sample C resulted in a secondary galvanic cell with aluminum being formed. This secondary galvanic cell increased the current density as well as corrosion rate, and led to reduction of its corrosion resistance more than two other samples.
- The corrosion tendency at each part of welded joints was less than aluminum, but it was higher than steel. In

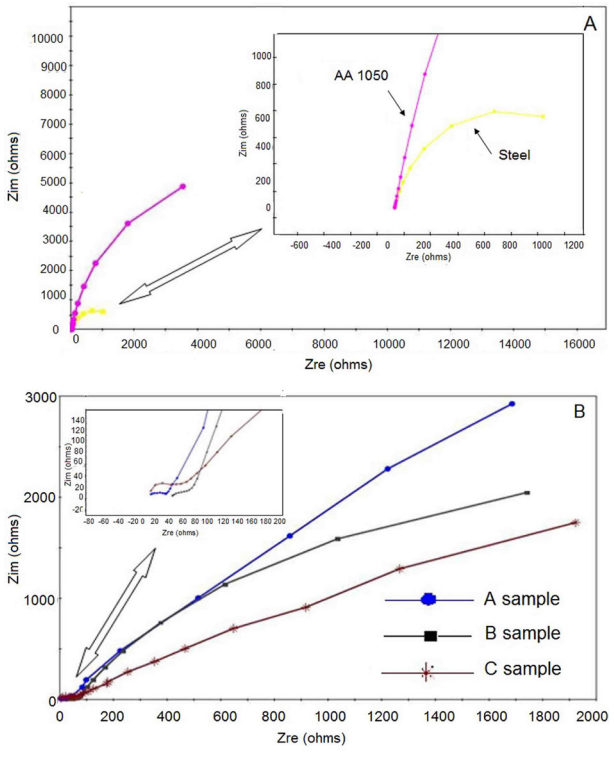

Fig. 9. Nyquist diagrams of electrochemical impedance (EIS), A: Raw aluminum and steel B: Welded samples.

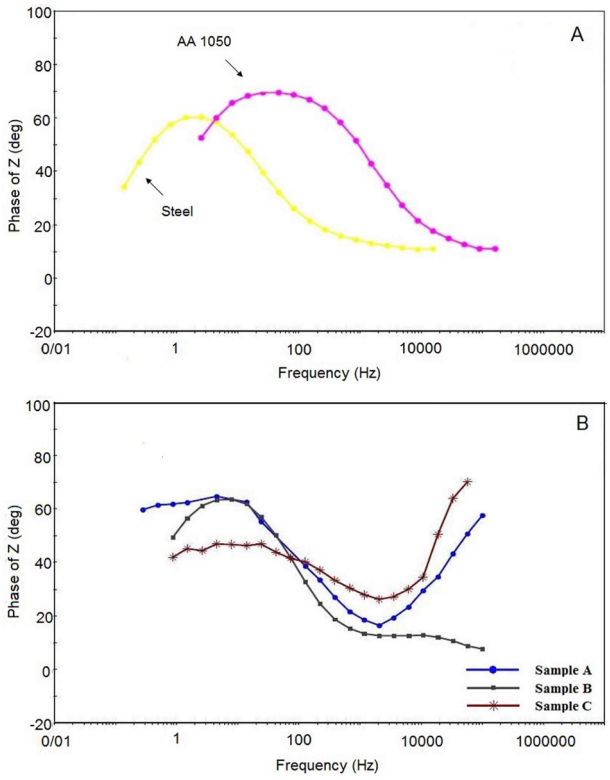

Fig. 10. BODE phase diagrams of electrochemical impedance (EIS), A: Raw aluminum and steel, B: Welded diagrams.

contrast, corrosion rate of the welded joints was lower than steel, but it was higher than aluminum.

- Sample A had the highest surface film resistance (R_F) and charged transfer resistance (R_{ct}). In other words, the lower value of iron phase at the aluminum/steel interface and the slighter tendency towards creating a galvanic cell resulted in a higher corrosion resistance.

References

[1] B. Crossland: Explosive Welding of Metals and Its Applications, Oxford University Press, New York, (1982).
[2] T. Z. Blazynski: Explosive Welding, Forming and Compaction, Applied Science Publishers, England, (1983).
[3] M. Benak, M. Turna, M. Ozvold, P. Nesvadba, J. Lokaj, L. Caplovic, F. Kovac and V. Stoyka: Roznov pod Radhostem Czech Republic, EU, (2010), 235.
[4] K. Raghukandan: J. Mater. Process. Tech., 139(2003), 573.
[5] N. Kengkla, N. Tareelap: Proc. Conf. 1stMae., Fah Luang University, Thailand, (2012).
[6] U. Kamachi Mudali, B. M. Ananda Rao, K. Shanmugam, R. Natarajan and B. Raj: J. Nucl. Mater., 321(2003), 40.
[7] M. Acarer: J. Mater. Eng. Perform., 21(2012), 2379.
[8] N. Kahraman and B. Gulenc: J. Mater. Process. Tech., 169(2005), 127.
[9] N. Kahraman and B. Gulenc: Int. J. Impact. Eng., 34(2007), 1423.
[10] H. R. Zareie Rajani, S. A. A. Akbari Mousavi and F. Madani Sani: Mater. Design., 43(2013), 467.
[11] ASTM E8M, Standard Test Methods for Tension Testing of Metallic Materials, Book of Standards, 03.01, USA, (2006).
[12] ASTM 384-11, Standard Test Method for Knoop and Vickers Hardness of Materials, Book of Standards, 03.01, USA, (2011).
[13] ASTM G1-03, Preparing, Cleaning, and Evaluating Corrosion Test Specimens, Book of Standards, (2003).
[14] M. L. Huang and L. Wang: Metall. Mater. Trans. A., 29(1998), 3037.
[15] R. V. Tamhankar and J. Ramesam: Mater. Sci. Eng., 13(1974), 245.
[16] S. A. A. Akbari Mousavi and P. FarhadiSartangi: Mater. Design., 30(2009), 459.
[17] G. H. Liaghat, S. A . Dehghan Manshadi: Modares Mechanical Engineering, 10(2010), 54.
[18] K. Hokamoto, T. Izuma, M. Fujita, M. Aoyagi: Welding Int., 6(1992), 941.
[19] S. A. A. Akbari Mousavi and S. T. S Al-Hassani: J. Mech. Phys. Solids., 53(2005), 2501.
[20] B. Gulenc: Mater. Sci. Eng., 29(2008), 275.
[21] F. Findik: Mater. Sci. Eng., 32(2011), 1081.
[22] A. M. A. Alsamuraee, H. A. Ameen and S. I. Jafer: J. Sci. Ind. Res., 51(2011), 283.
[23] S. A. Yahya and A. A. Rahim: Sains Malaysiana, 40(2011), 953.
[24] M. R. Khanzadeh Gharah Shiran, S. J. Mohammadi Baygi, S. R. Kiahoseyni, H. Bakhtiari and Allah M. Dadi: Int. J. Damage. Mech., (2016), 1.